

# Transition from a Mixotroph/Heterotroph Protist Community During the Dark Winter to a Photoautotrophic Spring Community in Arctic Surface Waters

Claudia Sabine Bruhn (✉ [claudia.bruhn@awi.de](mailto:claudia.bruhn@awi.de))

Alfred Wegener Institute

Nina Lundholm

Natural History Museum of Denmark, University of Copenhagen

Per Juel Hansen

University of Copenhagen

Sylke Wohlrab

Alfred Wegener Institute

Uwe John

Alfred Wegener Institute



---

## Research Article

**Keywords:** sea ice, succession patterns, metabarcoding, spring bloom formation, parasites, functional diversity, time series

**Posted Date:** October 8th, 2021

**DOI:** <https://doi.org/10.21203/rs.3.rs-951783/v1>

**License:**   This work is licensed under a Creative Commons Attribution 4.0 International License. [Read Full License](#)

---

# Abstract

Unicellular plankton communities (protists) are the basis of the marine food web. The spring bloom is especially important, because of its high biomass. However, it is poorly described how the protist community structure in Arctic surface waters develops from winter to spring. We show that mixotrophy and parasitism are the prominent trophic modes in the dark winter period. The transition period was characterized by a high relative abundance of mixotrophic dinoflagellates, while centric diatoms and the haptophyte *Phaeocystis pouchetii* dominated the successive phototrophic spring bloom event. Our observations indicate the presence of a characteristic winter community and a community shift from winter to spring, and not just a dormant spring community waiting for better circumstances. The spring bloom initiation commenced while sea ice was still obstructing the light penetration into the water column. The initiation coincided with a change in day length and spectral composition of the light, rather than with an increased light intensity. The initial increase in fluorescence, and therefore photosynthetic activity, was detected relatively deep in the water column, at ~55 m depth. This suggests that water column stratification and a complex interplay of abiotic factors eventually promote the spring bloom initiation.

## 1. Introduction

The Arctic is one of the fastest changing environments due to climate change [1-3]. This has already affected the Arctic biosphere, and will lead to further changes in the future [4]. The base of the complex marine pelagic food web consists of unicellular organisms, such as bacteria and eukaryotic unicellular plankton (protists) occupying different ecological niches, and providing the food source for higher trophic levels.

Because of their crucial role in the ecosystem, marine protists are frequent study subjects. Community studies of Arctic pelagic waters often focus on transect or snapshot studies [5-8], which do not properly display the temporal dynamics. The pelagic winter protist community in the Arctic has been characterized as most likely heterotrophic [9, 10] with phototrophic diatoms being present mostly in a stage of dormancy, e.g. as resting spores [11, 12].

The periods with ice cover have been declining during the past decades due to climate change and this is expected to impact the timing and dynamics of the spring bloom, and the trophic modes of the protist community [13, 14]. Phytoplankton blooms have occasionally been found to develop before the sea ice melts [15-17], and recent studies have recognized the abundance of parasitic and mixotroph protists in sea ice presence [18, 19]. The seeding of the pelagic phototrophic spring bloom event by sea ice algae has also been discussed, especially in relation to multiyear sea ice [20, 21]. While the pattern of phototroph dominance during the spring bloom event is comparably well-described [22, 33, 36], the community structure of the winter community and its transition towards the vernal bloom is less investigated [10], especially in relation to seasonal sea ice. To understand the link between the biosphere and climate change in an ecosystem such as the Arctic, it is important to understand the general biotic patterns and their interactions with their environment. Therefore, a study of how the marine protist community evolves from the winter composition to a spring bloom composition is necessary. With the presented work, we aim to discuss the impact of the occurrence of seasonal sea ice and other abiotic parameters in their interplay with the protist community structure transition, with special focus on the functional groups of the observed organisms.

## 2. Materials And Methods

### 2.1 Study site description and sampling procedure

Sampling was performed off the southern coast of Disko Island, West Greenland, close to the Arctic Station in Qeqertarsuaq. The area is characterized by coastal proximity, annual seasonal sea ice, and influence of the calving glacier Jakobshavn Isbræ. Samples were taken between February 10 and April 23, 2018 around noon. The sampling started at 69°12.95' N, 53°31.25' W, which had a water depth of approx. 140 m. As this location became inaccessible due to sea ice formation and growth, the sampling station was moved to 69°14.2' N, 53°29.9' W, depth: ca. 140 m, from March 16, 2018, approximately 2.5 km away from the first position. The alternative position was chosen as the best compromise between comparability to the first location and probable accessibility throughout the sampling period. The samples were taken approximately every four days with a 25 L Niskin water sampler (KC Denmark, Denmark) either from the water surface or through a manually drilled hole in the ice. The samples, taken at the depths 5 m, 10 m, 20 m, 30 m, and 40 m were transferred to polyethylene containers (pre-treated with 3 % hydrochloric acid and flushed twice with the respective sample), stored cold and dark, and processed on the same day.

## 2.2 Sea ice and contextual data

The water sampling was accompanied by an SBE 911plus CTD (Sea-Bird Scientific, Washington, USA) to collect temperature, photosynthetic active radiation (PAR), fluorescence and salinity data. For continuous environmental data above sea level, light from a station located at 69°15'12.558" N, 53°30'50.863" W, 25 m above sea level was provided by Greenland Environmental Monitoring (GEM) program, subprogram "GeoBasisDisko". Sea ice was observed both locally at the sampling location on the sampling day, and daily of the whole bay area by visual sea ice monitoring of the Arctic Station provided by the University of Copenhagen, Denmark.

## 2.3 Sample preparation and analysis

As biomass during the Arctic winter is rather low and sampling of larger volumes of water are logistically limited, we applied a pooling approach of the upper 40 m of the water column. Equal volumes (10 L) of water from five depths (5, 10, 20, 30 and 40 m) were pooled in order to obtain these depth-integrated samples. Data for Chlorophyll *a* (Chl *a*), and particulate organic carbon and nitrogen (POC and PON) as biomass and nutrition status proxies were retrieved from supplementary material of Bruhn *et al.* [37]. The following method of size fractionation might have impacted the integrity of more fragile cells, which could have fragmented under the pressure of the vacuum filtration. The reads of a few larger taxa such as *Strombidium* spp. (Fig. 4a) in the picoplankton size fraction may have been the result of this method. On the other hand, these findings could also hint at the presence of considerably smaller gametes. Overall, this method holds more scientific value than it has drawbacks, allowing e.g. insights in seasonal colony formation of the haptophyte *Phaeocystis pouchetii*, and was successfully applied in other field studies several times [53, 8, 37]. Therefore, the remaining 47.5 L pooled sample was size fractionated through a series of filters. Prefiltering through a 200 µm nylon mesh removed most multicellular zooplankton, also resulting in a loss of some larger protist species and colonies. Afterwards, the complete sample was filtered through a 20 µm nylon mesh to obtain the microplankton size fraction. Further filtration steps were carried out with polycarbonate filters and a vacuum pump at minimum -500 mbar, resulting in the filtration of 3 L through a 3 µm pore size (for obtaining the nanoplankton size fraction) and 1 L through a 0.2 µm pore size (for obtaining the picoplankton size fraction). The cells were carefully flushed off the surface of the filters. Afterwards, they were frozen in extraction buffer and transported for extraction in the home institution. The DNA from these three size fractions (0.2 – 3 µm or picoplankton, 3 – 20 µm or nanoplankton, 20 – 200 µm or microplankton) was extracted using a NucleoSpin Soil kit (Macherey-Nagel, Germany). The 16S rRNA Metagenomic Sequencing Library Preparation protocol (Illumina, California, USA) was used. However, the protocol was adapted with primers targeting the eukaryotic V4-region [54] modified to include haptophytes, which are otherwise mostly underrepresented when using the original primers [55]. Nevertheless, this method still tends to overestimate the abundance of dinoflagellates, because their genome usually displays a high copy number of ribosomal operons [56]. After sequencing 300 bp paired-end with a MiSeq System (Illumina, California, USA),

amplicon sequence variants (ASVs) were generated and annotated (as described in [57] and with the PR<sup>2</sup>-database; version 4.11.1; [58]). The species were marked with their respective trophic mode, if known, by manual curation (see table in supplementary data for applied criteria). Afterwards, the 50 most abundant ASVs from the taxonomic groups of dinoflagellates, haptophytes, cryptophytes, diatoms and ciliates were determined after excluding low abundance ASVs and non-protist ASVs. These ASVs were analyzed and their identity confirmed through phylogenetic placement.

For this, alignments with longer reference sequences of the different target groups (dinoflagellates, haptophytes, cryptophytes, diatoms, or ciliates) have been generated with MAFFT, using the L-INSI settings and the "--add-fragments --reorder" option. Afterwards, a phylogenetic tree was calculated with RAxML for 1000 bootstrap analyses, separately for dinoflagellates, haptophytes, cryptophytes, diatoms, and ciliates, respectively resulting in one maximum likelihood tree per taxonomic group. These trees served as a reference for the phylogenetic assignment or confirmation of the 50 most abundant ASV sequences of the aforementioned taxonomic groups. Alignments and resulting trees have been manual curated and analyzed.

Further analyses were performed with R, version 4.0.3 [59], with RStudio version 1.3.1093 [60], and the packages effects [61], eulerr [62], ggplot2 [63], lubridate [64], MBA [65], mgcv [66], phyloseq [67], plyr [68], RColorBrewer [69], reshape2 [70], tidyverse [71], and vegan [72]. Low abundance ASVs and non-protist ASVs were excluded. Read numbers were then normalized to average sequencing depth and afterwards set to 100 % reads, to be able to assess the relative abundance in context with biomass. To facilitate some analyses, the samplings were summarized into three phases divided by the calendar month they were taken in. This resulted in phase 1 from February 10 to 27 (containing five samplings), phase 2 from March 7 to 30 (containing five samplings), and phase 3 from April 5 to 23 (containing four samplings).

## 3. Results

### 3.1 Environmental observations

#### 3.1.1 Oceanographical context

The CTD measurements resulted in several depth profiles, of which photosynthetically active radiation (PAR), water density, chlorophyll fluorescence, and salinity are presented (Fig. 1). PAR measurements showed some penetration of light into the water at the beginning of the study up until March 7 and again from April 23 and onwards (Fig. 1a). Between these dates, there was almost no light penetrating into the water column. The measured density of the water column showed a slight shallowing of a few meters of the layers (Fig. 1d). Fluorescence values started to increase around March 30 at a depth of approximately 55 m (Fig. 1c). Additionally, it formed two layers at 40 m and 7 m depth between April 5 and April 9, respectively. Afterwards, on April 13, fluorescence was detected as deep as 100 m. Salinity values showed different layers in the water column, which shallowed over time (Fig. 1b).

#### 3.1.2 Sea ice presence

In the following, we distinguish between the overall sea ice presence in the entire bay area and sea ice directly at the sampling station. Sea ice was present, but did not cover the full bay throughout the whole period. In the Disko Bay area, the sea ice cover reached a maximum coverage of 99 % on February 12, and covered at least 75 % until April 25, when the ice slowly started to break up (Fig. 2a, black line). At the sampling station, sea ice was building up between March 7 and March 16 (Fig. 2a, white area), when it reached a thickness of more than 40 cm with an additional snow

cover. After April 5, the ice at the sampling station began to melt again, rendering the sampling on April 13 to be from the sea ice edge and the sampling on April 23 from the water surface.

### 3.1.3 Light

The day length increased during the sampling period, which therefore led to an increased total daily light intensity (Fig. 2b). The spectral composition of the light above the water also changed during the study (Fig. 2b). While incoming longwave radiation (4500 to 42000 nm wavelength) only experienced a slight increase in the daily average, incoming shortwave radiation (300 to 2800 nm wavelength) increased two to three times as much during the observed time period. The daily average of PAR increased even more rapidly, compared to longwave and shortwave radiation.

### 3.2 Community structure changes

Biomass data were represented as particulate organic carbon (POC), particulate organic nitrogen (PON) and chlorophyll *a* (Chl *a*). POC and PON were measured to 63.7  $\mu\text{g mL}^{-1}$  POC and 4.9  $\mu\text{g L}^{-1}$  PON on the first day of measurement (February 10), and decreased until 14.0  $\mu\text{g L}^{-1}$  POC on March 21 and 0.8  $\mu\text{g L}^{-1}$  PON on February 21 (Table 1). Afterwards, both POC and PON increased until the end of the sampling campaign to their highest values of 70.8  $\mu\text{g L}^{-1}$  POC (on April 23) and 12.7  $\mu\text{g L}^{-1}$  PON (on April 13). In contrast, Chl *a* gradually increased from almost unmeasurable with 0.01  $\mu\text{g L}^{-1}$  on February 21 to 1.26  $\mu\text{g L}^{-1}$  on April 19 (Figure 2a).

Table 1  
POC and PON as biomass proxies. Data were retrieved from Bruhn *et al.* [37].

|                              | Feb 10 | Feb 15 | Feb 21 | Feb 27 | Mar 07 | Mar 16 | Mar 21 | Mar 26 | Apr 05 | Apr 13 | Apr 19 | Apr 23 |
|------------------------------|--------|--------|--------|--------|--------|--------|--------|--------|--------|--------|--------|--------|
| POC [ $\mu\text{g L}^{-1}$ ] | 68.40  | 63.72  | 43.29  | 16.36  | 33.46  | 31.41  | 14.01  | 16.18  | 23.79  | 66.13  | 49.82  | 70.79  |
| PON [ $\mu\text{g L}^{-1}$ ] | 3.73   | 4.94   | 0.8    | 6.44   | 6.41   | 5.83   | 3.77   | 3.51   | 4.64   | 12.67  | 8.24   | 12.19  |

In total, 4,009 different ASVs were assigned to protists in the metabarcoding analyses. The 300 most abundant protist ASVs accounted for 81 to 98 % of all reads, depending on the sampling date, of which 97 % were present in all three monthly phases. On the other hand, ASVs that were unique to a certain month were the overall least abundant ASVs, ranging from 14.3 % (February exclusive ASVs) over 5.4 % (April exclusive ASVs) to 4.7 % (March exclusive ASVs) of all reads.

A range from 44.9 % in picoplankton, over 36.9 % in nanoplankton to 21.8 % in microplankton of all protist ASVs were shared among all three time phases (Fig. 3). The highest number of unique ASVs per month is detected in February and the smallest number in April.

In February, the protist communities in all size fractions were mostly heterotroph, parasitic and mixotroph. The percentage of ASVs linked to heterotrophic taxa declined strongly during the sampling period, whereas ASVs linked to phototrophic species increased with time leading to a phototroph dominated community in April (Fig. 4a). ASVs linked to phototrophic taxa were mainly diatoms, especially in the nanoplankton and microplankton size fractions. In picoplankton and nanoplankton, a considerable amount of reads initially accounted for parasitic protists, but were

displaced by mixotrophic protists in March and April. Over time, Shannon diversity declined in all size fractions (Fig. 4b). Picoplankton and nanoplankton have significantly different Shannon diversity indices between the three monthly phases (with ANOVA,  $F_{(2,12)} = 33.1$ ,  $p < 0.05$  for picoplankton and  $F_{(2,12)} = 16.6$ ,  $p < 0.05$  for nanoplankton), with significantly lower Shannon diversity indices in April compared to February and March, but no difference between February and March (Tukey adjusted p-values  $< 0.05$ ). In microplankton, the three monthly phases also differed significantly (ANOVA,  $F_{(2,12)} = 16.4$ ,  $p < 0.05$ ), with significantly lower Shannon diversity indices in April and March compared to February, but no difference between April and March (Tukey adjusted p-values  $< 0.05$ ).

When evaluating the 50 most abundant ASVs of ciliates, cryptophytes, diatoms, dinoflagellates (excluding Syndiniales), and haptophytes individually, the successional patterns of some putative species stand out (Fig. 5). In the following, the putative species belonging to the ASVs will be called by the respective species name assigned after phylogenetic placement analyses and are meant as presumed species names. Ciliates were diverse and difficult to identify to species level. Most noteworthy, one ASV of an unidentified heterotrophic tintinnid declined in abundance in the microplankton size fraction, accounting for  $> 20\%$  of all microplankton reads on February 12 to  $< 2\%$  on April 23 (Fig. 5a). Cryptophytes, which are either mixotrophs or phototrophs, were mainly found in the picoplankton size fraction. Here, *Teleaulax gracilis*, *Falcomonas daucooides* and the *Plagioselmis* stage of *Teleaulax amphioxeia* all increased in abundance with time (Fig. 5b).

The most abundant diatom in the microplankton size fraction was *Porosira glacialis*, followed by *Thalassiosira antarctica* var. *borealis*. In nanoplankton, the most abundant diatoms were *Chaetoceros gelidus*, *Navicula flagillifera* and other *Navicula* species. *Chaetoceros gelidus* had the highest relative abundance in February and March, declining with time. On the other hand, *Navicula flagillifera* and other *Navicula* spp. were the most relatively abundant diatoms towards the bloom initiation in April. *Skeletonema* sp. was the most important diatom of the picoplankton size fraction, and it increased in relative abundance during bloom initiation in April (Fig. 5c).

Overall, dinoflagellates made up the most abundant group based on absolute sequence read numbers. However, species groups have different amounts of rRNA copies per cell in their genomes and dinoflagellates are known to have particular high amounts of copy numbers, making a direct comparison across groups challenging, but this is less impacted when comparing within a group. All of the 50 most abundant dinoflagellate taxa are most likely constitutive mixotrophs and heterotrophs. In the picoplankton size fraction *Gymnodinium* spp. and *Karenia* sp. increased in relative abundance over time, whereas *Karlodinium* sp. stayed more or less at the same level throughout the study period. In the nanoplankton, *Gymnodinium* spp. neither increased nor decreased, while *Tripos* sp. and *Prorocentrum* sp. increased in the spring period, whereas *Karenia* sp. and *Gyrodinium* sp. decreased. In the microplankton size fraction, *Torodinium robustum* and *Tripos* sp. decreased in relative abundance. *Alexandrium ostenfeldii* was also a fairly abundant species in the microplankton size fraction, and was present throughout the whole sampling period, but had a very low relative abundance from April 9 on (Fig. 5d).

When analyzing haptophytes, a clade of six unidentifiable ASVs was found, which were distantly related to *Chrysochromulina* spp. The mixotroph or phototroph *Phaeocystis pouchettii* was the most prominent haptophyte. It increased in relative abundance over time in all three size fractions (existing both as single cells and in large colonies). In microplankton, *P. pouchettii* was almost non-existent until April 9, whereas in the nanoplankton fraction, it gradually increased in abundance and peaked on April 9 (Fig. 5e).

## 4. Discussion

The winter communities were dominated by parasites, heterotrophs and mixotrophs during February (Fig. 4a). In more temperate coastal regions, where more light is available, small heterotrophic protists are also dominating the winter population [23], showing that this may be a general strategy for winter communities. However, especially the picoplankton and nanoplankton size fractions revealed a high relative abundance of parasitic organisms during winter, and not only general heterotrophs. At times, the picoplankton fraction consisted almost entirely of parasites and heterotrophs, which underlines the importance of these two trophic modes for the winter community. Most marine parasitic protists are relatively small and target considerably larger cells as host organisms [24, 25], indicating that most of the parasitic protists detected in the study were most likely in their free-living stage, showing up in the picoplankton fraction. Very few parasites were detected in the microplankton fraction, further supporting the conjecture that few of the parasites were inside microplankton host cells, unless these cells were broken up by the filtration process. In Antarctic waters, parasitic protists have been detected as being surprisingly prevalent in winter [26], probably associated with the sea ice lead, i.e. long openings in the sea ice cover [18]. Parasitic protists usually do not stay alive for prolonged periods of time without their host organisms and they complete their free-living stages within a few hours to days [24, 27, 28]. Most of the parasitic organisms were dinoflagellates, specifically Syndiniales. Resting spores as an overwintering strategy for parasites have not been described yet, although such a strategy is a possibility [29]. Syndiniales often infect ciliates, dinoflagellates, cercozoons and crabs [29], i.e. groups of mixotrophic and heterotrophic organisms, but apparently not or only rarely diatoms [30]. In Disko Bay, heterotrophic and especially mixotrophic dinoflagellates were detected in all size fractions. The overall biomass (assessed as POC) was, however, extremely low (Table 1). Little is known about the autoecology of parasitic dinoflagellates in the ocean, in particular because of their difficult maintenance under laboratory conditions. The existing laboratory experiments suggest that they are not fit to live without their host organisms for an extended period of time [24, 28]. It is possible that the parasitic organisms observed were simply very successful in finding their host organisms and completing their life cycles with an output of many new individual cells (dinospores), but we cannot exclude alternative survival strategies. The presence of mixotrophic organisms, mainly constitutive mixotrophs, may be related to them having had an advantage over organisms which are less flexible in their trophic mode, because they gain energy from both harvesting the little light available and additional food uptake.

Also later, during the early stages of the spring bloom, mixotrophs, especially dinoflagellates (CMs), contributed substantially to the total photosynthetic protist community in the pico- and nanoplankton size fractions (March, phase 2). This may have been a response to the slightly increased day length (Fig. 2b), although the light reaching into the water was still negligible (Fig. 1a). Similar observations in the community structure have recently been made in the Young Sound fjord in Northeast Greenland. Here, a bloom of mixotrophic haptophytes developed in ice covered surface waters during early spring [19]. The two locations differ considerably with regard to salinity and nutrient concentrations. Nevertheless, mixotrophs seemed to have had an advantage at both locations, because they compensate for low levels of photosynthesis with their ability to ingest other organisms. The mixotrophic ability seems to give them the flexibility to quickly adapt to increasing light availability, thereby giving them an advantage over pure photoautotrophs at this seasonal time point. It is even possible that mixotrophy dominates the pelagic food web during much of the year in the Arctic, due to this increased persistence [74].

April (phase 3) marked the initiation of the spring bloom. The spring bloom community was mainly characterized by photosynthetic diatoms, especially in the nanoplankton and microplankton size fractions. In the dark winter period in the Arctic, the primary source of energy for phototrophs is naturally lacking, while other nutrients are sufficient. One possible overwintering strategy for diatoms are resting spores, which can germinate when the conditions are more favorable [31-33]. Another strategy for fast adaptation to better conditions of phototrophs, mainly diatoms, is the quick photosynthetic reactivation of resting cells after a period of darkness, as resting cells only display a much-

reduced metabolic rate [34]. The presence of diatoms throughout all phases, albeit in small proportions, also reflected by low Chl *a* measurements (Fig. 2a), suggests the utilization of the latter or both strategies. As stated before, diatoms are usually not the primary target of the parasitic Syndiniales. Thus, diatoms seem to combine the advantages of the ability to photosynthesize, being r-strategists, surviving as resting cells and with not being targeted by parasitic organisms, possibly giving them the critical advantage for overgrowing the other organisms both proportionally and in absolute abundance, leading to the spring bloom event.

Diatoms are typical spring bloom organisms and are often the dominant taxa in Arctic spring blooms [22, 35-37]. The genera, *Thalassiosira* spp. and *Navicula* spp. have previously been detected as important spring bloom species in the Baffin Bay area, not far from the sampled position, albeit much later in the year and two years prior in 2016 [36]. *Porosira glacialis* is also a cold-water diatom, commonly found in the northern hemisphere [38, 39], and was also one of the dominating phototrophs in the microplankton size fraction (Fig. 5c).

*Phaeocystis* spp. are often abundant in Arctic surface waters during the early spring where the surface waters are still covered by sea ice [9, 40]. *Phaeocystis* spp. are often regarded as a climate altering species, because they are able to produce dimethylsulfide [41, 42]. They are considered a less desirable food source for zooplankton compared to other phytoplankton taxa [43, 44]. Interestingly, in our study, *P. pouchetii*, seemed to start as solitary cells in phase 1 and 2 (in the picoplankton fraction) making them potential prey for microplankton (Fig. 5e). Later in phase 3, towards the bloom, this species started to form larger colonies. The colony formation observed here may have been a defense mechanism against smaller copepod species [44]. However, larger copepods, such as *Calanus* spp., are typically occurring in larger quantities just around the spring bloom event [73], and can subsequently graze on these colonies. *Phaeocystis* spp. have an advantage over diatoms, because they are not dependent on silicate concentrations, which diminish quickly during the spring bloom [37]. Compared to some other Arctic phytoplankton species, *Phaeocystis* spp. have a wider tolerance towards temperature, as they are also commonly found in the Atlantic [45]. This increased fitness makes them a possible candidate for gaining importance in the spring bloom event in the future. We can confirm presence of *P. pouchetii* in the Arctic winter community, as also shown close to Svalbard [46], underlining a considerable resilience in harsh conditions.

The diversity analyses showed that the community in winter was generally more diverse than towards and during the spring bloom event (Fig. 4b). Interestingly, the smaller the organisms, the more similar the phases were in terms of presence or absence of ASVs (Fig. 3). The largest differences were thus seen in the microplankton size fraction, in which only 21.8 % of ASVs were shared among all size fractions. These findings are similar to a comparative study of ASVs from Iceland and Greenland [8], in which the microplankton size fraction was most dissimilar compared to smaller size fractions. Locally adapted populations of larger celled species are discussed to have lower flexibility and to be more plastic than smaller cells, which might differentiate more rapidly into distinct ecotypes, giving them some adaptational flexibility [8, 75]. Therefore, these cells may be viewed as more specialized in the different phases, resulting in a more drastic community shift. In a global context, it has been shown that the highest phytoplankton diversity often is detected at intermediate biomasses, while especially high and low biomass correlate with lower diversity [47]. In our case, we found that the low biomass winter community was surprisingly diverse (Fig. 3b) and that the diversity, by means of ASVs and Shannon diversity index, decreased with the onset of the spring bloom. This suggests a highly diverse winter community followed by a spring bloom, in which only few diatom ASVs started to dominate the community in both relative and absolute abundance, as the conditions became favorable for them. Additionally, the overall less diverse microplankton size fraction reacted quicker by means of community shifts to a changing environment than the smaller size fractions, again supporting the hypothesis that larger celled species react quicker to environmental changes due to higher niche specificity.



Studies in the Arctic have been investigating the phytoplankton spring bloom both in areas with sea ice [17, 48] and without sea ice [10]. The ice cover has often been discussed as a factor involved in the initiation of the spring bloom because snow and ice cover will lower the penetration of light into the water column, depriving phototrophs of their energy source [48, 20]. However, the transition from a sea ice covered surface water environment to surface waters without sea ice cover has rarely been studied. Here, we present data on the bloom dynamics starting in the dark winter period to the breakage of the sea ice and formation of a spring bloom. The slow increase in Chl *a* unmistakably shows the initiation of the spring bloom event at a time when the sea ice was still largely covering the Bay (Fig. 2a). Biomass is, at this time, not yet strongly increasing, but when taking POC into consideration, the amount of phototrophs (measured as Chl *a*) is increasing in relation to the total amount of biomass, showing the imminence of the spring bloom (Fig. 2a, Table 1).

A number of publications have shown that phytoplankton growth is possible under very low light conditions, as often observed in surface waters under the sea ice [15-17]. It has also been shown that once the light penetrates the ice, photosynthetic capabilities are quickly reactivated, usually within a few hours to a day [34]. In the present study, the light penetrating the ice was extremely limited at the time of increasing photosynthetic activity (Fig. 1a, c), while the spectral light quality and the average insolation per day above water changed considerably (Fig. 2b). It is well known that the wavelength is also influenced by possible and variable cloud cover [49], but the overall tendency of the wavelength shifts were clearly seen in the daily averages of the light intensity in the present study (Fig. 2b). Shortwave radiation that penetrates water deeper than longwave radiation, increased more strongly during this period. This suggests that light quality and average light irradiation per day in combination may be more important for bloom initiation than the light intensity itself. Low light intensity can possibly be compensated for by longer light duration and different wavelength composition. Still, it is standing out that the fluorescence measurement shows that the bloom started at a depth of approximately 55 m, which coincided with the approximate halocline at that time (Fig. 1b, c). The early start of ice algal blooms initiating directly under the sea ice has been discussed previously [20], but our study suggests that the pelagic spring bloom was not seeded from the sea ice or from the bottom of the sea ice as pennate diatoms typically dominate sea ice communities. Instead, we observed typical centric pelagic bloom species, similar to the findings of Arrigo *et al.* [50, 51]. In combination with the depth of the developing bloom, this does not suggest a seeding of the bloom by sea ice algae. Apart from that, it is possible that the breakage of the sea ice could have led to increased turbulences in the upper ocean layers. This could help non-motile cells such as diatoms to stay in the illuminated layers of the ocean, increasing the amount of possibly absorbed photons due to residence in lighter areas of the ocean, eventually enabling their growth. During the initiation of the spring bloom, the local area was still completely covered with sea ice. However, open patches further away from the sampling area may have been sufficient to increase the mixing in the suggested way and to lead to advective effects.

## Conclusion

During winter, the protistan community mostly consisted of parasites, heterotrophs, and mixotrophs, which is probably a natural adaptation to a life at low light availability [18, 19]. The transitional period was characterized by a high relative abundance of mixotrophs, which most likely have a trophic advantage due to their flexibility. The community shift towards a spring bloom community already started before the sea ice retreated. Past studies have forecasted and shown an increase in primary productivity when the sea ice retreats, based on satellite data [51, 52]. However, *in situ* studies, such as ours, confirm that blooms of microbial plankton not only occur [15, 16, 17, 19, 40], but also start growing while ice is still covering the surface waters. We also show that the period prior to the phytoplankton spring bloom is most likely not a period of dormancy, but only a period of low biomass, because changes in the community are still occurring. This suggests that sea ice retreat is not the major factor of initiating the

phytoplankton spring bloom in the Arctic. Rather, an interplay of the factors of light intensity, spectral composition and day-length, as well as oceanographic factors such as nutrient availability and mixed layer depth are involved, making the spring bloom initiation and the shift from the winter community a multifactorial event.

## Declarations

### Acknowledgements

Our thanks go to Nancy Kühne for providing technical assistance in the laboratory. We also thank Regin Rønn, Kjeld Akaraaq Mølgaard, Abel Brandt, and Johannes Mølgaard for their help on location during the field campaign in Greenland. The expedition was conducted within the framework of the Disko Marine Basis Program. The POC and PON analyses were done with Florian Koch, who we thank for his support. Claudia Sabine Bruhn and Uwe John were financially and logistically supported through the PACES II research program of the Alfred Wegener Institute, Helmholtz Centre for Polar and Marine Research. The Ministry for Science and Culture of Lower Saxony and the Volkswagen Foundation through the “Niedersächsisches Vorab” grant program (grant number ZN3285) provided funding for Sylke Wohlrab. The Danish Research Council for Nature and Universe (9040-00248B) provided funding to Nina Lundholm. The Danish Ministry of the Environment provided funding for Per Juel Hansen and Nina Lundholm through the Marine Basis Disko Program as part of the Greenland Environmental Monitoring Program (GEM).

### Author contributions

C.S.B., N.L., and U.J. planned the study. C.S.B. coordinated and performed the sampling and processing of the samples, the analysis of the samples as well as most of the analysis of the data. U.J. produced the phylogenetic placement of the most abundant ASVs. P.J.H. and C.S.B. assigned trophic modes to the different ASVs. S.W. and C.S.B. wrote the scripts for analyzing the data. S.W. performed statistical analyses. All authors interpreted the resulting data. C.S.B. wrote the manuscript and prepared the graphs. The supplementary material was also prepared by C.S.B. The manuscript was revised by S.W., P.J.H., N.L., and U.J. All authors reviewed the final manuscript before submission and confirmed its originality.

### Competing Interests

No competing interests has been declared by the authors.

## References

1. Overpeck, J. *et al.* Arctic Environmental Change of the Last Four Centuries. *Science***278**, 1251–1257 (1997).
2. McBean, G. *et al.* Arctic Climate: Past and Present. *Arct. Clim. Impact Assess.* 21–60 (2005).
3. Pachauri, R. K., Reisinger A. (Eds., Core Writing Team). IPCC: Climate Change 2007: Synthesis Report. Contribution of Working Groups I, II and III to the Fourth Assessment Report of the Intergovernmental Panel on Climate Change. IPCC, Geneva, Switzerland, 104 pp. (2007).
4. Hoegh-Guldberg, O. & Bruno, J. F. The Impact of Climate Change on the World’s Marine Ecosystems. *Science***328**, 1523–1529 (2010).
5. Baggesen, C. *et al.* Molecular phylogeny and toxin profiles of *Alexandrium tamarense* (Lebour) Balech (Dinophyceae) from the west coast of Greenland. *Harmful Algae***19**, 108–116 (2012).

6. Tillmann, U., Kremp, A., Tahvanainen, P. & Krock, B. Characterization of spiroside producing *Alexandrium ostenfeldii* (Dinophyceae) from the western Arctic. *Harmful Algae***39**, 259–270 (2014).
7. Elferink, S. *et al.* Molecular diversity patterns among various phytoplankton size-fractions in West Greenland in late summer. *Deep. Res. Part II***121**, 54–69 (2017).
8. Elferink, S. *et al.* Comparative Metabarcoding and Metatranscriptomic Analysis of Microeukaryotes Within Coastal Surface Waters of West Greenland and Northwest Iceland. *Front. Mar. Sci.***7**, 1–20 (2020).
9. Marquardt, M., Vader, A., Stübner, E. I., Reigstad, M. & Gabrielsen, T. M. Strong Seasonality of Marine Microbial Eukaryotes in a High-Arctic Fjord (Isfjorden, in West Spitsbergen, Norway). *Appl. Environ. Microbiol.***82**, 1868–1880 (2016).
10. Kubiszyn, A. M. *et al.* The annual planktonic protist community structure in an ice-free high Arctic fjord (Adventfjorden, West Spitsbergen). *J. Mar. Syst.***169**, 61–72 (2017).
11. Zhang, Q., Gradinger, R. & Spindler, M. Dark Survival of Marine Microalgae in the High Arctic (Greenland Sea). *Polarforschung***65**, 111–116 (1998).
12. Hegseth, E. N. & Tverberg, V. Effect of Atlantic water in flow on timing of the phytoplankton spring bloom in a high Arctic fjord (Kongsfjorden, Svalbard). *J. Mar. Syst.***113–114**, 94–105 (2013).
13. Alexander, V. & Niebauer, H. J. Oceanography of the eastern Bering Sea ice-edge zone in spring. *Limnol. Oceanogr.***26**, 1111–1125 (1981).
14. Hunt Jr., G. L. *et al.* Climate change and control of the southeastern Bering Sea pelagic ecosystem. *Deep. Res. Part II***49**, 5821–5853 (2002).
15. Arrigo, K. R. *et al.* Under Arctic Sea Ice. *Science***336**, 1408 (2012).
16. Spall, M. A. *et al.* Deep-Sea Research II Role of shelfbreak upwelling in the formation of a massive under-ice bloom in the Chukchi Sea. *Deep. Res. Part II***105**, 17–29 (2014).
17. Massicotte, P. *et al.* Green Edge ice camp campaigns: understanding the processes controlling the under-ice Arctic phytoplankton spring bloom. *Earth System Sci. Data***12**, 151–176 (2020).
18. Clarke, L. J., Bestley, S., Bissett, A. & Deagle, B. E. A globally distributed Syndiniales parasite dominates the Southern Ocean micro-eukaryote community near the sea-ice edge. *ISME J.***13**, 734–737 (2019).
19. Sjøgaard, D. H. *et al.* An under - ice bloom of mixotrophic haptophytes in low nutrient and freshwater - influenced Arctic waters. *Sci. Rep.***11**, 1–9 (2021).
20. Leu, E. *et al.* Arctic spring awakening – Steering principles behind the phenology of vernal ice algal blooms. *Prog. Oceanogr.***139**, 151–170 (2015).
21. Olsen, L. M. *et al.* The seeding of ice algal blooms in Arctic pack ice: The multiyear ice seed repository hypothesis. *J. Geophys. Res. Biosci.***122**, 1529–1548 (2017).
22. Tammilehto, A., Watts, P. C. & Lundholm, N. Isolation by Time During an Arctic Phytoplankton Spring Bloom. *Eukaryot. Microbiol.***64**, 248–256 (2017).
23. Morán, X. A. G., Calvo-díaz, A., Arandia-Gorostidi, N. & Huete-Stauffer, T. M. Temperature sensitivities of microbial plankton net growth rates are seasonally coherent and linked to nutrient availability. *Environ. Microbiol.***20**, 3798–3810 (2018).
24. Alacid, E., Reñé, A. & Garcés, E. New Insights into the Parasitoid *Parvilucifera sinerae* Life Cycle: The Development and Kinetics of Infection of a Bloom-forming Dinoflagellate Host. *Protist***166**, 677–699 (2015).
25. Gómez, F., Moreira, D. & López-García, P. Life cycle and molecular phylogeny of the dinoflagellates *Chytriodinium* and *Dissodinium*, ectoparasites of copepod eggs. *Eur. J. Protistol.***45**, 260–270 (2009).

26. Cleary, A. C. & Durbin, E. G. Unexpected prevalence of parasite 18S rDNA sequences in winter among Antarctic marine protists. **38**, 401–417 (2016).
27. Reñé, A., Alacid, E., Figueroa, R. I., Rodríguez, F. & Garcés, E. Life-cycle, ultrastructure, and phylogeny of *Parvilucifera corolla* sp. nov. (Alveolata, Perkinsozoa), a parasitoid of dinoflagellates. *Eur. J. Protistol.***58**, 9–25 (2017).
28. John, U. *et al.* An aerobic eukaryotic parasite with functional mitochondria that likely lacks a mitochondrial genome. *Sci. Adv.***5**, 1–11 (2019).
29. Guillou, L. *et al.* Widespread occurrence and genetic diversity of marine parasitoids belonging to Syndiniales (Alveolata). *Environ. Microbiol.***10**, 3349–3365 (2008).
30. Tillmann, U., Hesse, K.-J. & Tillmann, A. Large-scale parasitic infection of diatoms in the Northfrisian Wadden Sea. *J. Sea Res.***42**, 255–261 (1999).
31. McQuoid, M. R. & Hobson, L. A. Importance of resting stages in diatom seasonal succession. **50**, 44–50 (1995).
32. Tsukazaki, C., Ishii, K., Matsuno, K., Yamaguchi, A. & Imai, I. Distribution of viable resting stage cells of diatoms in sediments and water columns of the Chukchi Sea, Arctic Ocean. *Phycologia***57**, 440–452 (2019).
33. Luostarinen, T. *et al.* An annual cycle of diatom succession in two contrasting Greenlandic fjords: from simple sea-ice indicators to varied seasonal strategists. *Mar. Micropaleontol.***158**, 1–15 (2020).
34. Kvernvik, A. C. *et al.* Fast Reactivation of Photosynthesis in Arctic Phytoplankton during the Polar Night. *Phycol. Soc. Am.***54**, 461–470 (2018).
35. Krause, J. W. *et al.* Biogenic silica production and diatom dynamics in the Svalbard region during spring. *Biogeosciences***15**, 6503–6517 (2018).
36. Lafond, A. *et al.* Late spring bloom development of pelagic diatoms in Baffin Bay. *Elem. Sci. Anthr.***7**, 1–24 (2019).
37. Bruhn, C. S., Wohlrab, S., Krock, B., Lundholm, N. & John, U. Seasonal plankton succession is in accordance with phycotoxin occurrence in Disko Bay, West Greenland. *Harmful Algae***103**, 101978 (2021).
38. McMinn, A., Pankowski, A. & Delfatti, T. Effect of Hyperoxia on the Growth and Photosynthesis of Polar Sea Ice Microalgae. *J. Phycol.***41**, 732–741 (2005).
39. Svenning, J. B., Dalheim, L., Eilertsen, H. C. & Vasskog, T. Temperature dependent growth rate, lipid content and fatty acid composition of the marine cold-water diatom *Porosira glacialis*. *Algal Res.***37**, 11–16 (2019).
40. Pavlov, A. K. *et al.* Altered inherent optical properties and estimates of the underwater light field during an Arctic under-ice bloom of *Phaeocystis pouchetii*. *J. Geophys. Res. Ocean.***122**, 4939–4961 (2017).
41. Stefels, J. & van Boeckel, W. H. M. Production of DMS from dissolved DMSP axenic cultures of the marine phytoplankton species *Phaeocystis* sp. *Mar. Ecol. Prog. Ser.***97**, 11–18 (1993).
42. Verity, P. G. *et al.* Current understanding of *Phaeocystis* ecology and biogeochemistry, and perspectives for future research. *Biogeochemistry***83**, 311–330 (2007).
43. Weisse, T., Tande, K., Verity, P., Hansen, F. & Gieskes, W. The trophic significance of *Phaeocystis* blooms. *J. Mar. Syst.***5**, 67–79 (1994).
44. Nejstgaard, J. C. *et al.* Zooplankton grazing on *Phaeocystis*: a quantitative review and future challenges. *Biogeochemistry***83**, 147–172 (2007).
45. Hoppe, C. J. M., Wolf, K. K. E., Schuback, N., Tortell, P. D. & Rost, B. Compensation of ocean acidification effects in Arctic phytoplankton assemblages. *Nat. Clim. Chang.***8**, 529–533 (2018).

46. Vader, A., Marquardt, M., Meshram, A. R. & Gabrielsen, T. M. Key Arctic phototrophs are widespread in the polar night. *Polar Biol.***38**, 13–21 (2015).
47. Irigoien, X., Huisman, J. & Harris, R. P. Global biodiversity patterns of marine phytoplankton and zooplankton. *Lett. to Nat.***429**, 863–867 (2004).
48. Terrado, R., Lovejoy, C., Massana, R. & Vincent, W. F. Microbial food web responses to light and nutrients beneath the coastal Arctic Ocean sea ice during the winter – spring transition. *J. Mar. Syst.***74**, 964–977 (2008).
49. Kapsch, M.-L., Graversen, R. G., Tjernström, M. & Bintanja, R. The Effect of Downwelling Longwave and Shortwave Radiation on Arctic. *Am. Meteorol. Soc.* 1143–1159 (2016). doi:10.1175/JCLI-D-15-0238.1
50. Arrigo, K. R. *et al.* Journal of Geophysical Research: Oceans. *J. Geophys. Res. Ocean.***122**, 9350–9369 (2017).
51. Arrigo, K. R., van Dijken, G. & Pabi, S. Impact of a shrinking Arctic ice cover on marine primary production. *Geophys. Res. Lett.***35**, 1–6 (2008).
52. Renaut, S., Devred, E. & Babin, M. Northward Expansion and Intensification of Phytoplankton Growth During the Early Ice-Free Season in Arctic. *Geophys. Res. Lett.***45**, 10,590-10,598 (2018).
53. Krock, B., Tillmann, U., John, U. & Cembella, A. D. Characterization of azaspiracids in plankton size-fractions and isolation of an azaspiracid-producing dinoflagellate from the North Sea. *Harmful Algae***8**, 254–263 (2009).
54. Stoeck, T., Bass, D., Nebel, M., Christen, R. & Meredith, D. Multiple marker parallel tag environmental DNA sequencing reveals a highly complex eukaryotic community in marine anoxic water. *Mol. Ecol.***19**, 21–31 (2010).
55. Piredda, R. *et al.* Diversity and temporal patterns of planktonic protist assemblages at a Mediterranean LTER site. *FEMS Microbiol. Ecol.***93**, 1–14 (2017).
56. Guo, L., Sui, Z. & Liu, Y. Quantitative analysis of dinoflagellates and diatoms community via Miseq sequencing of actin gene and v9 region of 18S rDNA. *Sci. Rep.* 1–9 (2016). doi:10.1038/srep34709
57. Sprong, P. A. A. *et al.* Spatial dynamics of eukaryotic microbial communities in the German Bight. *J. Sea Res.***163**, 1–15 (2020).
58. Guillou, L. *et al.* The Protist Ribosomal Reference database (PR<sup>2</sup>): a catalog of unicellular eukaryote Small Sub-Unit rRNA sequences with curated taxonomy. *Nucleic Acids Res.***41**, 597–604 (2012).
59. R Core Team. R: A language and environment for statistical computing. *Stat. Comput. Vienna, Austria* (2020).
60. R Team. RStudio: Integrated Development Environment for R. *PBC, Boston, MA*
61. Fox, J. & Weisberg, S. An R Companion to Applied Regression, 3rd Edition. *Thousand Oaks, CA* (2019).
62. Larsson, J. eulerr: Area-proportional Euler and Venn Diagrams with Ellipses. R package version 6.1.0.
63. Wickham, H. ggplot2: Elegant Graphics for Data Analysis. *Springer-Verlag, NY* (2016).
64. Golemund, G. & Wickham, H. Dates and Times Made Easy with lubridate. *J. Stat. Softw.***40**, 1–25 (2011).
65. Finley, A., Banerjee, S. & Hjelle, Ø. MBA: Multilevel B-Spline Approximation. R package version 0.0-9. (2017).
66. Wood, S. N., Pya, N. & Saefken, B. Smoothing parameter and model selection for general smooth models (with discussion). *J. Am. Stat. Assoc.***111**, 1548–1575 (2016).
67. McMurdie, P. J. & Holmes, S. phyloseq: An R package for reproducible interactive analysis and graphics of microbiome census data. *PLoS One***8**, e61217 (2013).
68. Wickham, H. The Split-Apply-Combine Strategy for Data Analysis. *J. Stat. Softw.***40**, 1–29 (2011).
69. Neuwirth, E. RColorBrewer: ColorBrewer Palettes. R package version 1.1-2. (2014).
70. Wickham, H. Reshaping Data with the reshape Package. *J. Stat. Softw.***21**, 1–20 (2007).
71. Wickham, H. Welcome to the tidyverse. *J. Open Source Softw.***4**, 1686 (2019).

72. Oksanen, J. *et al.* vegan: Community Ecology Package. R package version 2.5-6. (2019).
73. Møller, E. F. & Nielsen, T. G. Borealization of Arctic zooplankton – smaller and less fat zooplankton species in Disko Bay, Western Greenland. 1175–1188 (2020).
74. Stoecker, D. K. & Lavrentyev, P. J. Mixotrophic Plankton in the Polar Seas: A Pan-Arctic Review. *Front. Mar. Sci.* **5**, 1–12 (2018).
75. Wohlrab, S. *et al.* Metatranscriptome Profiling Indicates Size-Dependent Differentiation in Plastic and Conserved Community Traits and Functional Diversification in Dinoflagellate Communities. *Front. Mar. Sci.* **5**, 1–13 (2018).

## Figures

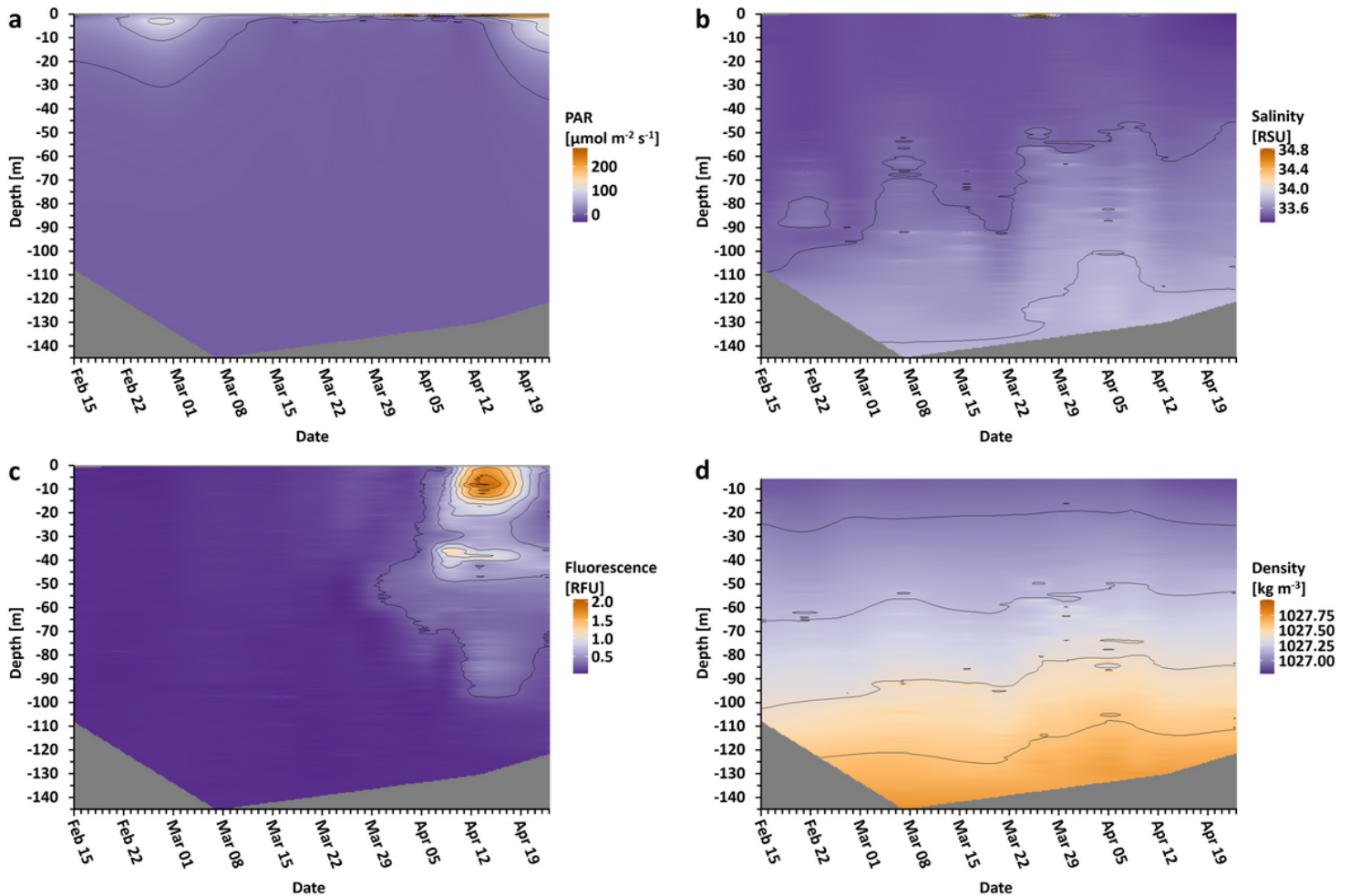


**Figure 1**

Oceanographic data in depth profile over time. Depicted are photosynthetic active radiation (a, PAR), salinity (b), fluorescence (c), and the density of the water (d). Isolines are displayed for orientation regarding the different values. Grey areas indicate unmeasured depths.

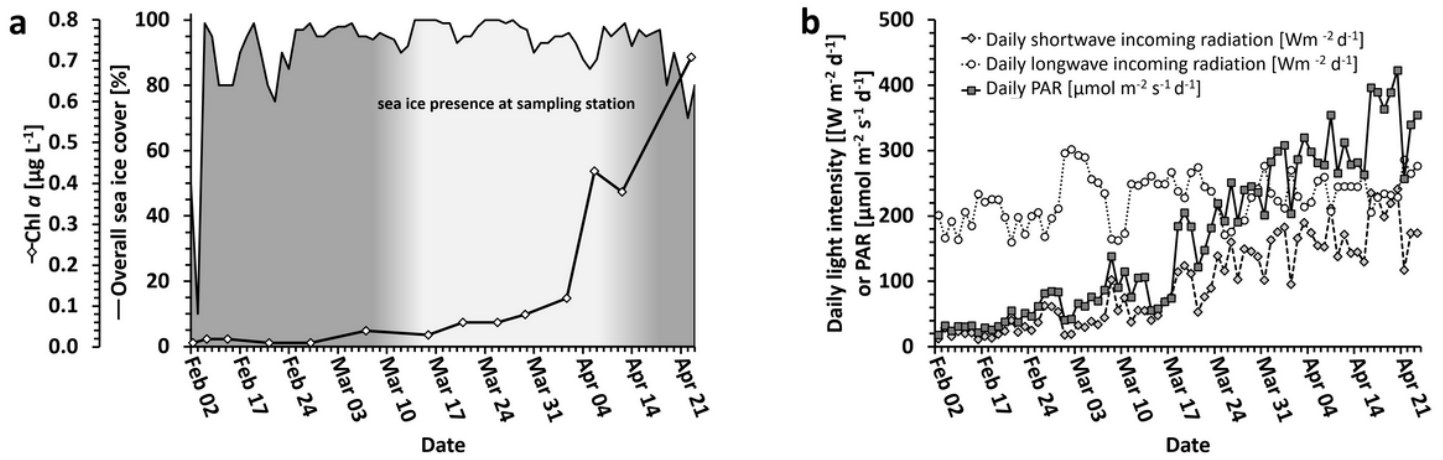


**Figure 2**

Light and ice conditions. a: Local photosynthetic biomass (solid line with diamonds) in relation to sea ice coverage (solid line). The sea ice coverage of the entire bay area is shown as a black line. The sea ice at the sampling station is indicated as the white coloring below the line. b: Light quality change over time above water. Incoming longwave radiation and incoming shortwave radiation as well as PAR are displayed as daily averages.

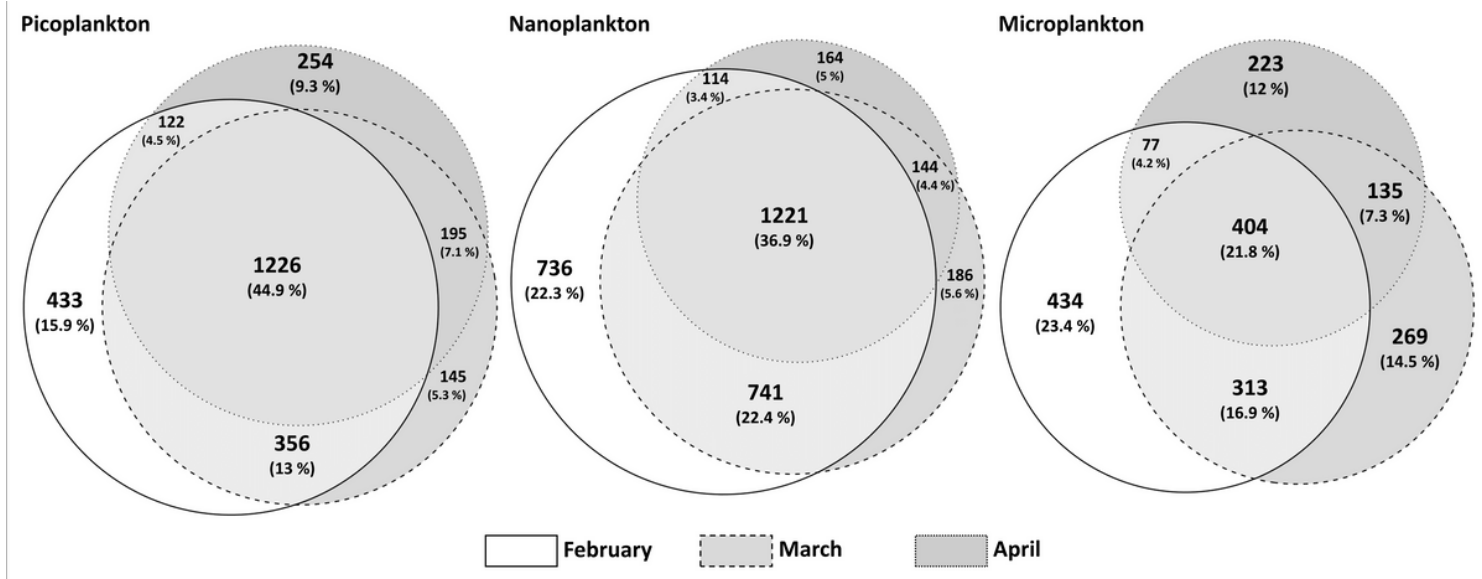


**Figure 3**

Venn-Diagram adaptation of ASVs per monthly phase and size fraction. A presence/absence-matrix was the basis for this visualization, where shared ASVs per calendar month are depicted in the overlaps. The circles are proportional to the number of unique ASVs.

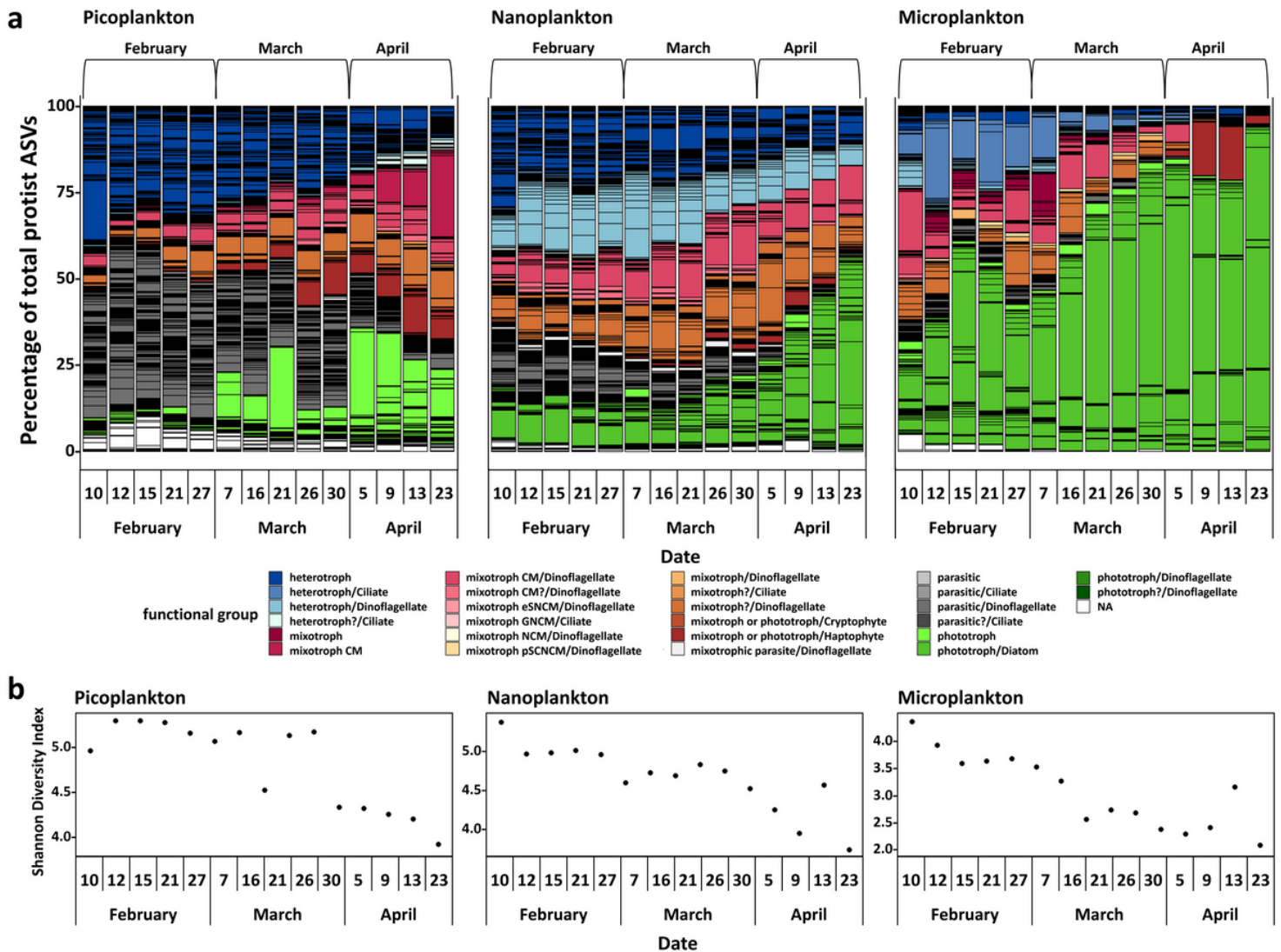


**Figure 4**

Protist community analyses. Normalized protist ASVs, divided by functional group and size fraction and additionally divided into three phases by calendar month (a). CM=constitutive mixotroph, eSNCM=endo-symbiotic specialist non-constitutive mixotrophs, GNCM=generalist non-constitutive mixotrophs, NCM=non-constitutive mixotroph, pSNCM=plastidic specialist non-constitutive mixotrophs. It was not possible to assign the definite trophic mode to each ASV, hence a putative trophic mode (indicated with a question mark or NA) is displayed. The Shannon Diversity Index (b) is also displayed.



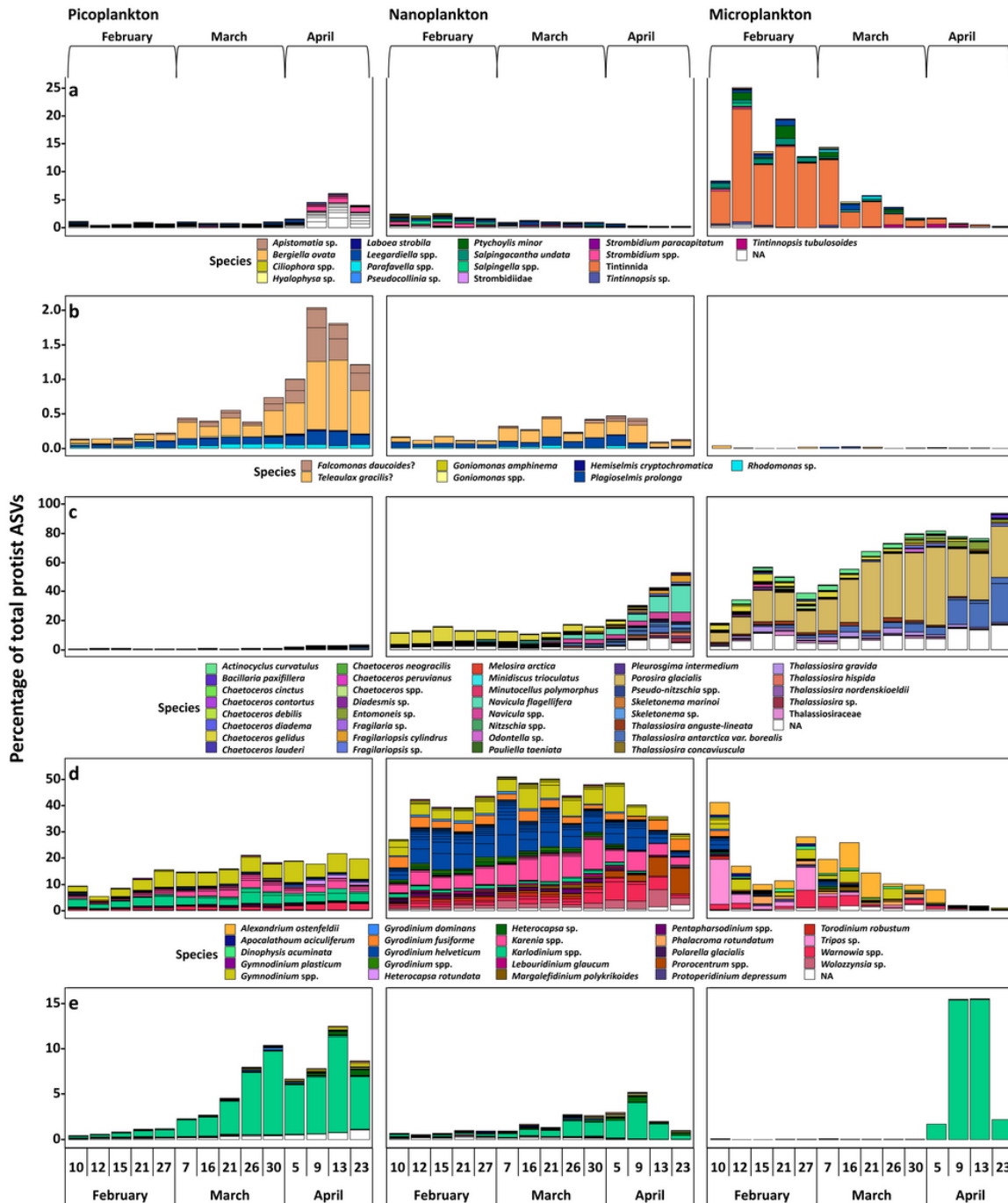


Figure 5

most important ASVs of the taxonomic groups of ciliates (a), cryptophytes (b), diatoms (c), dinoflagellates, excluding Syndiniales (d), and haptophytes (e). Displayed are a maximum of the 50 most abundant ASVs, if applicable. Each species name is to be understood as putative, as the species themselves were not confirmed via microscopic investigation but only through phylogenetic placement.

## Supplementary Files

This is a list of supplementary files associated with this preprint. Click to download.

- [Assignedtrophicmode.docx](#)

- [ASVtable.xlsx](#)
- [CTDdata.xlsx](#)
- [Ciliatesphylogeneticplacement.pdf](#)
- [Cryptophytesphylogeneticplacement.pdf](#)
- [Diatomsphylogeneticplacement.pdf](#)
- [Dinoflagellatesphylogeneticplacement.pdf](#)
- [Haptophytesphylogeneticplacement.pdf](#)